Ship Propulsion Plant Transient Response Investigation using a Mean Value Engine Model

Gerasimos P. Theotokatos

Abstract—In the present paper, the transient response of a merchant ship propulsion plant is investigated using a model implemented in the computational environment MATLAB/Simulink. The main engine of the vessel, which is considered to be of the two-stroke marine Diesel type, is modeled by the means of a quasi steady cycle mean value approach. According to that, two non-linear first order differential equations, which are derived by applying the angular momentum conservation in engine crankshaft and turbocharger shaft, are used for the calculation of engine crankshaft and turbocharger shaft rotational speeds. The other engine operating parameters are calculated after the solution of a non-linear algebraic system of three equations corresponding to the mass and energy balances in the engine components. In order to calculate the propeller thrust and torque, the polynomials for the propellers of the Wageningen B type are used. In addition, the ship velocity and the movement along its longitudinal axis are also calculated using the differential equation describing the ship surge dynamics. The engine model is validated against previously published experimental data. Then, the simulation of merchant ship propulsion plant under various operating conditions is performed and the derived results are presented and discussed.

Keywords— Mean value engine modeling, Ship propulsion plant, Simulation, Two-stroke marine Diesel engine.

I. Introduction

PROPULSION of the vast majority of merchant ships utilizes marine Diesel engines as prime movers. A typical propulsion plant of a merchant ship include a single, slow speed turbocharged, two-stroke marine Diesel engine directly coupled via the shafting system to a single, fixed pitch propeller [1], [2]. Although a merchant ship propulsion plant is designed based on the steady state performance characteristics of its components [1], [2], a great amount of time of the propulsion plant operation is spent under dynamic conditions throughout the ship lifetime. In that respect, the understanding of the transient response of the ship propulsion plant is of essential importance in order to elucidate the complex interactions occurring between the propulsion plant components. The costs for the procurement and operation of a merchant ship propulsion plant installation are extremely high and therefore, the accomplishment of extensive measuring campaigns in order to experimentally investigate its dynamic behavior would be prohibited. Instead, simulation tools are used for propulsion plant transient response investigations as well as throughout the development and optimization procedure of the ship powerplant components.

The simulation tools used for the propulsion plant engine transient response studies are categorized as cycle mean value models and zero or one-dimensional models. The representation of the real engine processes is enhanced as the complexity of the used simulation tool is increased (i.e. from cycle mean value models to one-dimensional models), but at the same time, greater amount of input data is required, the model execution time lasts longer and the model usage becomes more laborious. The cycle mean value models have the ability to represent the engine behavior with sufficient accuracy, whilst requiring limited amount of input data and quite reasonable time of execution [3], [4]. The basic assumption used in cycle mean value modeling approaches is that the air and fuel flows entering the engine cylinders are continuous and therefore the intermittent nature of engine operating cycle is neglected. In that respect, cycle mean value models can provide the engine cycle averaged temporal evolution of the engine operating parameters, whereas their in-cycle variation (e.g. per degree of crank angle) cannot be calculated. The mean value engine modeling approaches are divided in two groups: the quasi-steady ones, in which no mass accumulation is considered between the engine components [5], and the ones where modeling of engine receivers are additionally implemented [3], [4].

Previous studies concerning the development of cycle mean value engine models for two-stroke marine Diesel engines were reported in [6]–[11]. Studies of marine propulsion plants transient response investigation were presented in [12]–[23]. Transient cases of propulsion plants comprising four-stroke marine Diesel engines were investigated using either zero-dimensional models in [15], [19]–[20] or mean value models in [12], [21], [23]. Investigations of the transient behavior of propulsion plants with two-stroke marine Diesel engines using zero-dimensional simulation, which requires a considerable number of input data, were presented in [13]–[14], [16] –[18]. In [22], a cycle mean value model was used for the investigation of the transient behavior of a tanker propulsion plant during ice braking conditions, but a number for its required input data were produced using a zero-dimensional engine simulation code.

G. P. Theotokatos is Assistant Professor in the Department of Naval Architecture at Technological Educational Institute (TEI) of Athens, Ag. Spyridonos Str., Egaleo, GR-12210 GREECE (e-mail: mtheot@teiath.gr).

The objective of this work is to investigate the transient response of the overall propulsion plant of a bulk carrier vessel. In that respect, the mathematical modeling of the overall ship propulsion plant installation, implemented in the computational environment MATLAB/Simulink is used. The main engine of the ship propulsion plant is modeled using a quasi steady cycle mean value engine modeling approach. The engine crankshaft and turbocharger shaft speeds are calculated by solving two first order differential equations derived applying the angular momentum conservation in engine/propeller and turbocharger shafts, respectively. By applying the energy and mass conservation in the engine components, a non-linear algebraic system comprising as variables the air mass flow rate and the exhaust receiver gas pressure and temperature is derived. After the solution of that system the remaining engine variables are calculated. The ship velocity is calculated by solving a first order differential equation derived using the ship surge dynamics. The required propeller toque and thrust are calculated using the polynomials for the Wageningen B propeller type. Simulation of a two-stroke engine is performed, so that the model is validated based on previously published experimental data. Then, the simulation of the bulk carrier propulsion plant under various operating conditions is performed and the derived results are presented and discussed.

II. Propulsion plant Description

The typical propulsion plant installation of a modern merchant vessel, shown in Fig.1, consists of the main marine Diesel engine, the shafting system and the propeller. The main engine can be of the two-stroke type for installations of high power or of the four-stroke type for installations of lower power [2], [24]. In both cases, the engine is turbocharged by one or more turbocharger units so that the power produced by the engine is maximized. The shafting system comprises the connecting shafts and the bearings. For the cases where the main engine is of the four-stroke type, one gear box is connected between the engine crankshaft and the propeller shaft. In high power installations, a shaft generator is often installed in order to produce the required by the ship electric power during ship voyages, where the engine operates at relatively high load.

In the case of merchant vessels propulsion plant installation, the propeller is usually of fixed pitch type, although during the last years designs with controllable pitch propellers have also been used [25].

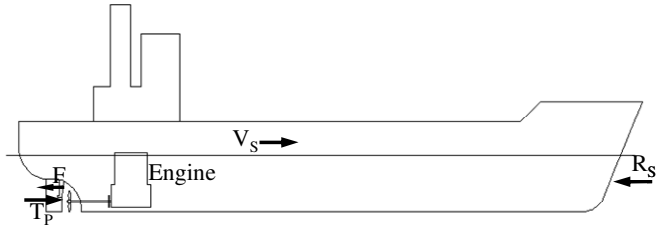

Fig. 1 Ship propulsion schematic

A. Cycle Mean Value Modeling of Two-Stroke Marine Diesel Engine

The cycle mean value modeling of the two-stroke marine Diesel engine is accomplished by considering the processes occurring in the engine components. The main engine components that have been mathematically modeled, shown in Fig. 2, are the cylinders, the scavenging and exhaust receivers, the compressor and turbine of the turbocharger and the engine air cooler. In addition, models for the engine exhaust pipe the engine speed governor are also used.

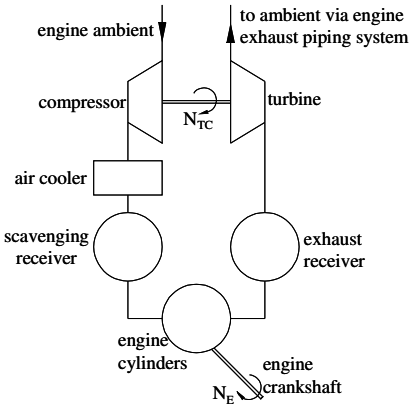

Fig. 2 Components of the two-stroke marine Diesel engine used for cycle mean value modeling

The engine crankshaft and turbocharger shaft speeds are calculated using the following equations derived by applying the angular momentum conservation in the propulsion plant shaft system and the turbocharger shaft, respectively:

$$\frac{dN_E}{dt} = \frac{30\left(\eta_{Sh} Q_E - Q_P\right)}{\pi\left(I_E + I_{Sh} + I_P + I_{ew}\right)} \tag{1}$$

$$\frac{dN_{TC}}{dt} = \frac{30\left(Q_T - Q_C\right)}{\pi I_{TC}} \tag{2}$$

The energy balance applied on engine cylinders gives:

$$(\dot{m}_a h_{SC} + \eta_{comb}\dot{m}_f H_L \zeta)\eta_{ex} = \dot{m}_e h_{ER} \tag{3}$$

where, ζ is fuel chemical energy proportion in the exhaust gas entering turbine [26] and η_{ex} is a correction factor used to take into account the heat transfer from the exhaust gas to the ambient in the cylinder exhaust ports and exhaust receiver.

The air and gas properties are considered to be constant. Thus, the temperature of the working medium (air or gas) throughout the engine components is calculated using the following equation:

$$h = c_p T \tag{4}$$

Combining eq. (3) and (4), the following relation is derived:

$$(\dot{m}_a c_{pa} T_{SC} + \eta_{comb}\dot{m}_f H_L \zeta)\eta_{ex} = \dot{m}_e c_{pe} T_{ER} \tag{5}$$

The proportion of the fuel chemical energy contained in the exhaust gas is considered linear function of the engine brake mean effective pressure [26]:

$$\zeta = k_{z0} + k_{z1}\overline{p}_b \tag{6}$$

The engine brake mean effective pressure is calculated by subtracting the friction mean effective pressure from the indicated mean effective pressure, i.e.:

$$\overline{p}_b = \overline{p}_i - \overline{p}_f \tag{7}$$

The indicated mean effective pressure is calculated using the rack position, the maximum indicated mean effective pressure of the engine and the combustion efficiency, which in turn is regarded as function of engine air to fuel ratio [27], [28]:

$$\overline{p}_i = x_r \overline{p}_{i,\max} \eta_{comb} \tag{8}$$

The friction mean effective pressure is considered function of the indicated mean effective pressure and the engine crankshaft speed [9]–[11]:

$$\overline{p}_f = k_{f0} + k_{f1} N_E + k_{f2} \overline{p}_i \tag{9}$$

By applying the mass balance in the engine cylinders, he following equation is derived:

$$\dot{m}_a + \dot{m}_f = \dot{m}_e \tag{10}$$

The engine cylinders of a two-stroke marine Diesel engine are modeled considering a system comprising two orifices connected in series. Each one of the orifices represents the cylinder intake ports and exhaust valve, respectively. These two orifices can be combined in one equivalent orifice, which produces the same mass flow rate for a given pressure ratio across engine cylinders. The equivalent orifice geometric area can be estimated using the areas of intake ports and exhaust valves, as follows [26]:

$$A_{eq} = \frac{z_{cyl}}{2\pi} \int_0^{2\pi} \frac{A_i(\phi) A_e(\phi)}{\sqrt{A_i^2(\phi) A_e^2(\phi)}} \mathrm{d}\phi \tag{11}$$

The cylinders air mass flow rate is calculated using the following equation, which has been derived according to the quasi-one dimensional consideration in an orifice with subsonic flow [27], [28]:

$$\dot{m}_a = c_d A_{eq} p_{SC} / \sqrt{R_a T_{SC}} \; f\left(pr_{cyl}, \gamma_\alpha\right), \quad pr_{cyl} = p_{ER} / p_{SC},$$
$$f\left(pr_{cyl}, \gamma_\alpha\right) = \sqrt{\left[2\gamma_\alpha / \left(\gamma_\alpha - 1\right)\right]\left(pr_{cyl}^{\,2/\gamma_\alpha} - pr_{cyl}^{\,(\gamma_\alpha+1)/\gamma_\alpha}\right)} \tag{12}$$

The engine exhaust gas mass flow rate is calculated by the following equation derived applying a quasi-one dimensional approach in the turbine [27], [28]:

$$\dot{m}_e = A_{T,eff} \frac{p_{ER}}{\sqrt{R_e T_{ER}}} \sqrt{\frac{2\gamma_e}{(\gamma_e - 1)}\left(pr_T^{2/\gamma_e} - pr_T^{(\gamma_e+1)/\gamma_e}\right)}$$
$$with \;\; pr_T = \max\left[p_{T,d} / p_{ER}, \left(2/(\gamma_e + 1)\right)^{\frac{\gamma_e}{\gamma_e - 1}}\right] \tag{13}$$

The turbine effective flow area is calculated from the turbine geometric area and the turbine flow coefficient. The turbine flow coefficient and efficiency are derived from turbine steady state performance maps and are considered polynomial functions of the turbine pressure ratio, i.e.:

$$A_{T,eff} = \alpha_T A_{T,geo}, \;\; \alpha_T = f(pr_T), \;\; \eta_T = f(pr_T) \tag{14}$$

The pressure after the turbine is calculated using the pressure increase of the exhaust piping system, which in turn is regarded as proportional to the exhaust gas mass flow rate squared:

$$p_{T,d} = p_{atm} + \Delta p_{ep} = p_{atm} + k_{ep} \dot{m}_e^2 \tag{15}$$

The engine fuel mass flow rate is calculated using the following equation, where of the injected fuel mass per cylinder and per cycle ($m_{f,cy}$) vs. fuel rack position is provided as input:

$$\dot{m}_f = z_{cyl} m_{f,cy} N_E / \left(60\, rev_{cy}\right) \tag{16}$$

The pressure and temperature of the air contained in the scavenging receiver are calculated by modeling the compressor and the air cooler. The compressor is usually modeled using its performance map. However, in marine propulsion plant systems, the engine is loaded according to the propeller law and the compressor operating points under steady state conditions lay on a single curve on the compressor map [13], [28], [29]. Depending on the selected surge margin, the compressor operating points could be located on regions of constant efficiency or close to the optimum compressor efficiency parabola. In that respect, the compressor pressure ratio can be modeled as function of the turbocharger shaft speed, whereas the compressor efficiency can be taken either as constant or on the optimum efficiency curve of the compressor map. In this work, the compressor pressure ratio and efficiency are regarded as second order polynomial functions of the turbocharger shaft speed and are calculated using the following equations:

$$pr_C = 1 + k_{C1} N_{TC} + k_{C2} N_{TC}^2 \tag{17}$$

$$\eta_C = k_{Cef0} + k_{Cef1} N_{TC} + k_{Cef2} N_{TC}^2 \tag{18}$$

The temperature of the air exiting compressor is calculated using the following equation, which has been derived using the compressor efficiency definition equation [28]:

$$T_C = T_{atm}\left(1 + \left(pr_C^{\,(\gamma_a - 1)/\gamma_a} - 1\right) / \eta_C\right) \tag{19}$$

The pressure and temperature of the air contained in the engine scavenging receiver are derived as follows:

$$T_{SC} = T_C\left(1 - \varepsilon_{AC}\right) + \varepsilon_{AC} T_{w,AC} \tag{20}$$

$$p_{SC} = p_C - \Delta p_{AC} = pr_C\, p_{atm} - \Delta p_{AC} \tag{21}$$

The air cooler effectiveness is assumed to be a polynomial function of the air mass flow rate, according to the following equation:

$$\varepsilon_{AC} = k_{AC0} + k_{AC1} \dot{m}_a + k_{AC2} \dot{m}_a^2 \tag{22}$$

The pressure drop in the air cooler is calculated by:

$$\Delta p_{AC} = f_{AC}\left(\rho_{AC} v_{AC}^2 / 2\right) = f_{AC} \dot{m}_a^2 / \left(2 \rho_{AC} A_{AC}^2\right) \tag{23}$$

Combining the equations (5)-(23), for a given set of engine speed, turbocharger shaft speed and engine governor rack position, (N_E, N_{TC}, x_r), a non-linear algebraic system is solved to obtain the following three independent variables: the air mass flow rate, the exhaust receiver gas pressure and the exhaust receiver gas temperature. Then, the remaining engine parameters are calculated from the respective equations given above.

In addition, the engine torque, power, brake specific fuel consumption and efficiency are calculated using the following equations:

$$Q_E = \frac{\overline{p}_b V_D}{2\pi\, rev_{cy}}, \; P_b = \frac{Q_E \pi N_E}{30}, \; bsfc = \frac{\dot{m}_f}{P_b}, \; \eta_b = \frac{P_b}{\dot{m}_f H_L} \tag{24}$$

The absorbed compressor impeller and delivered turbine wheel torques, required in eq. (2), are calculated by the following equations, respectively:

$$Q_C = \frac{P_C}{\pi N_{TC}/30} = \frac{\dot{m}_a c_{pa}\left(T_C - T_{atm}\right)}{\pi N_{TC}/30} \quad (25)$$

$$Q_T = \frac{P_T}{\pi N_{TC}/30} = \frac{\dot{m}_e c_{pe}\left(T_{ER} - T_{T,d}\right)}{\pi N_{TC}/30} \quad (26)$$

The temperature of the exhaust gas exiting turbine is calculated using the following equation, which is derived using the turbine efficiency definition equation [28]:

$$T_{T,d} = T_{ER}\left(1-\eta_T\left[1-\left(p_{T,d}/p_{ER}\right)^{\frac{\gamma_e-1}{\gamma_e}}\right]\right) \quad (27)$$

The engine governor is modeled using a proportional-integral (PI) controller law. Thus, the engine governor rack position is calculated as follows:

$$x_r = x_{r,o} + k_p \Delta N + k_i \int_0^t \Delta N dt \quad (28)$$

where $\Delta N = N_{ord} - N_E$ is the difference between the ordered engine speed and the actual engine speed. In addition, torque and scavenging pressure limiters have been also incorporated in the engine governor model as proposed and used by engine manufacturers for protecting the engine integrity during fast transients [16].

B. Propeller Modeling

The torque and thrust of the ship propeller, either of fixed or controllable pitch type, are calculated using the non-dimensional coefficients of torque and thrust respectively, as follows:

$$Q_P = k_Q \rho_{sw} N_P^2 D_P^5 \quad (29)$$

$$T_P = k_T \rho_{sw} N_P^2 D_P^4 \quad (30)$$

The non-dimensional coefficients of torque and thrust are calculated using the polynomial equations for the Wageningen B propeller type [30]:

$$k_Q = \sum CQ_{s,t,u,v} J^s \left(p/D_P\right)^t \left(A_E/A_o\right)^u z_P^v \quad (31)$$

$$k_T = \sum CT_{s,t,u,v} J^s \left(p/D_P\right)^t \left(A_E/A_o\right)^u z_P^v \quad (32)$$

In the above relations, the number of propeller blades, z_P, the disk area coefficient, A_E/A_o, the pitch to diameter ratio, p/D_P, and the propeller advance coefficient, J, are required as input. Provided that the propeller of the ship has been selected, the first two parameters are constant. In addition, for a fixed pitch type propeller, the pitch to diameter ratio also takes constant value. For the case of a controllable pitch propeller, the p/D_P values can vary according to a predetermined schedule or by the propeller pitch control system. The propeller advance coefficient, J, depends on the speed of advance (velocity of the water arriving in the propeller), V_A, the propeller rotational speed and the propeller diameter, according to the following equation:

$$J = \frac{V_A}{N_P D_P/60} \quad (33)$$

The speed of advance is calculated using the ship velocity and the ship wake fraction, w, which is considered constant taking values in the range from 0.20 to 0.45 for ships with a single propeller [30], [31]:

$$V_A = (1-w)V_S \quad (34)$$

The propeller open water efficiency is defined by the following relation:

$$\eta_P = k_T J/\left(k_Q 2\pi\right) \quad (35)$$

In order to take into account the inertia of the entrained water by the propeller, the entrained water coefficient, which, in turn, is presumed function of the propeller blades angle of attack [32], is used:

$$I_{ew} = \eta_{ew} I_P \quad (36)$$

The propeller blades angle of attack is derived as the difference between the blades geometric pitch angle and the angle of relative velocity at propeller blades leading edge (advance angle):

$$\alpha = \arctan\left(\frac{p/D_P}{\pi}\right) - \arctan\left(\frac{V_A}{V_u}\right) \quad (37)$$

The circumferential blade velocity is given by:

$$V_u = 0.7 D_P \left(\pi N_P/60\right) \quad (38)$$

The propeller real slip ratio [30], which is a parameter used in order to indicate the propeller loading under various operating conditions, is calculated by:

$$SR_R = 1 - \frac{V_A}{p\,N_P/60} \quad (39)$$

In the case where engine modeling is only of interest, i.e. the propeller and ship models will not be used, the propeller torque, required in eq. (1), is calculated according to the propeller law through the engine maximum continuous rating (MCR) operating point, as follows:

$$Q_P = k_P N_E^2,\ k_P = Q_{E,MCR}/N_{E,MCR}^2 \quad (40)$$

C. Ship Longitudinal Movement Modeling

By applying the ship surge dynamics, the following differential equation is derived for the calculation of the longitudinal ship velocity:

$$\left(m_S + m_{hydro}\right)\frac{dV_S}{dt} = T_P - F - R_S \quad (41)$$

The ship resistance, R_S, is considered a second order function of the ship velocity, V_S [24]. The mass, m_S, is the mass of the ship, which is calculated by multiplying the ship displacement with the sea water density. The term, m_{hydro}, is an added virtual mass, which is used in order to take into account the hydrodynamic force arising due to the acceleration of a body in a fluid [30].

The thrust deduction, F, is calculated using the thrust deduction coefficient, t, as given below:

$$F = t T_P \quad (42)$$

The thrust deduction coefficient can be taken as constant with typical values in the range from 0.12 to 0.30 for ships with a single propeller [31], or alternatively it can be presumed

as a function of ship velocity.

III. MODEL IMPLEMENTATION IN MATLAB/SIMULINK ENVIRONMENT

The mathematical modeling of the ship propulsion plant components, which was presented above in this text, was implemented in the MATLAB/Simulink environment, as shown in Fig. 3. The propulsion plant model consists of the following types of blocks: a) the blocks where the inputs of the submodels must be inserted, b) the blocks where the initial values of the engine crankshaft speed, the turbocharger shaft speed and the ship velocity have to be set, c) the blocks where the integration of the model differential equations of the model is performed, d) the blocks where the calculation of the parameters of the ship propulsion plant components is carried out, e) the ordered engine speed schedule block, f) the engine governor block and g) the output block of the model.

The required input data for the propulsion plant modeling are categorized in the following groups: the geometric data of the components, the properties of working media (air, exhaust gas, sea water) and the constants of the submodels.

The calculation procedure takes place as follows. At the start of the simulation time, the values for the three independent variables (air mass flow rate, exhaust receiver gas pressure and temperature) are estimated. For each time step, taking into account the values for the engine speed, turbocharger shaft speed and the ship speed (their initial values are taken into consideration at the start of the simulation time), the required parameters of the submodels are calculated and the non-linear algebraic system of the three variables are solved using the "fsolve" function of the Optimization Toolbox of MATLAB [33]. Having the air mass flow rate, the exhaust receiver gas pressure and temperature calculated, the remaining engine parameters as well as the time derivatives of the engine crankshaft speed and the turbocharger shaft speed are also derived. The last two parameters and the time derivative of the ship velocity are fed to the integration blocks, where the engine crankshaft speed, the turbocharger shaft speed and the ship velocity, are calculated, respectively, using a fourth order Runge-Kutta integration method with fixed time step. The above described procedure is repeated for every time step till the end of the simulation time.

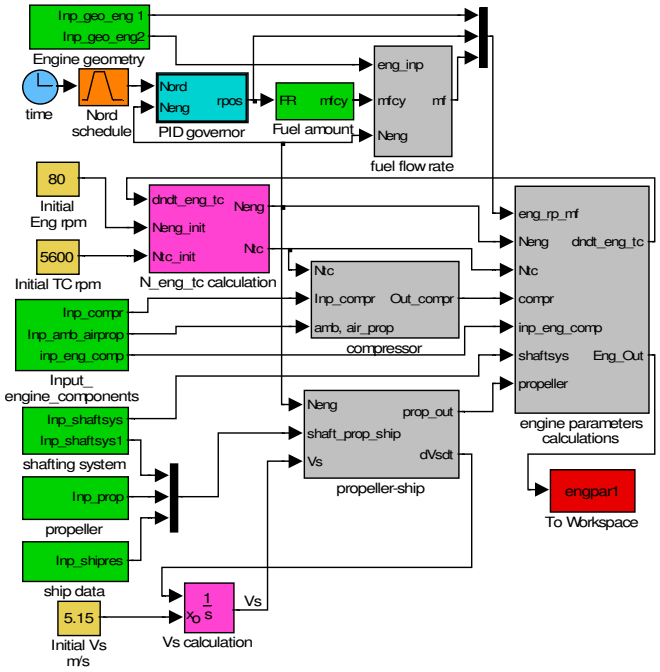

Fig. 3 Ship propulsion plant model implemented in MATLAB/Simulink

For each time step, a set of parameters of the ship propulsion plant is stored in a variable available to the workspace of MATLAB, so that the plots of the parameters variation can be easily constructed.

For the case of simulating only the two-stroke marine Diesel engine, a modified version of the model shown in Fig. 3 was also implemented, in which eq. (40) is used for the calculation of propeller torque.

IV. RESULTS AND DISCUSSION

In order to examine the ability of the above described mean value engine model for predicting the engine operating parameters with sufficient accuracy, the MAN B&W 4L60MC engine was simulated. That engine is of the two-stroke marine Diesel type, turbocharged by one turbocharged unit working on constant pressure turbocharging system. For that type of engine, experimental data under steady state and transient operating conditions were previously published in [13]. Part of those data is also used in Fig. 4 and 5 presented below, indicated as "reference". The main engine characteristics as well as the required model input data were extracted from the engine manufacturer project guide [34], whereas the required compressor and turbine input data were taken from [13]. The engine main parameters are given in Table I.

First, the model was set up providing the required input data. Then, simulation runs of the engine steady state operating conditions at 50%, 75%, 90% and 100% of the engine brake power were performed. Slight adjustments were performed in a number of the model variables, e.g. the engine cylinders discharge coefficient or turbine equivalent area, so that the model predictions are in acceptable agreement with the reference experimental data. The model predictions for a set of engine operating parameters including the brake mean effective pressure, the exhaust receiver gas temperature, the turbocharger shaft rotational speed and the scavenging receiver pressure are presented in Fig. 4. In the same figure, the respective measured data taken from [13] are also shown. As it can be inferred by comparing the data presented in Fig. 4,

TABLE I: ENGINE PARAMETERS

Engine type	4L60MC	
Number of cylinders	4	
Bore	600	mm
Stroke	1944	mm
Brake Power (MCR)	6720	kW
Engine speed (MCR)	111	rpm
bmep (MCR)	16.5	bar
Turbocharger units	1 MAN B&W NA57/TO	

the model predictions under engine steady state conditions exhibit adequate accuracy.

The next step was to examine the model ability to capture the engine transient response. In that respect, the Run 11 presented in [13] was simulated. According to that, engine abrupt load changes from 97% to 67% at the 5th s and back to 97% at the 38th s were demanded. Those correspond to changes in engine speed from about 110 rpm to 95 rpm. Such load changes are considered very fast and are usually avoided in real engine operation, but engine transient response under similar conditions are used for the control system design.

The transient run was initially performed by using the constants derived from the steady state runs, and the actual value of the turbocharger rotating parts polar moment of inertia. The analysis of the derived simulation results, which are not presented in this text, showed good agreement between simulation and measurements for engine speed and power variations, whereas the predictions for turbocharger speed, scavenging receiver pressure and exhaust gas receiver temperature varied more rapidly than the respective measured data. That was attributed to the unmodeled dynamics of engine scavenging air and exhaust gas receivers and the turbocharging system piping volumes, as it is also reported in [10]. The transient run was repeated using for the turbocharger rotating part polar moment of inertia its actual value increased by 100%, so that the dynamics of the engine receivers and turbocharger system volume are taken into account. A set of the derived simulation results, including the engine speed and brake power, the turbocharger speed, the scavenging receiver pressure and the exhaust receiver gas temperature, as well as the respective measured data (taken from [13]) are presented in Fig. 5. As it is deduced by comparing the simulation results to the respective measured data, the presented engine operating parameters (except for exhaust receiver gas temperature) are predicted with very satisfactory accuracy. Although the exhaust receiver gas temperature is adequately predicted under steady state conditions as it is shown in Fig. 4 and Fig. 5 (time periods: from the 1st s the 5th s, from the 25th s to the 38th s and from the 60th s to the 80th s), the model is not capable to capture the exhaust gas receiver response during engine fast transients (Fig. 5 time periods: from the 5th s to the 20th s and from the 38th s to the 60th s). To adequately predict the exhaust gas temperature variation during fast transients, a more detailed model, which should include the engine exhaust gas receiver modeling by means of the open thermodynamic system concept, is required, as it is explained in [10]. However, in cases of slow engine transients, which are usual for the ship propulsion plant operation, the engine operating parameters are predicted with enough accuracy using the modeling approach presented above in this text [10].

Having validated the engine model, the propulsion plant of a typical merchant ship was simulated. The ship taken into consideration was of the bulk carrier type having deadweight 55000 t. The ship propulsion plant consists of a MAN B&W 6L60MC engine (the same engine type as presented in Table I,

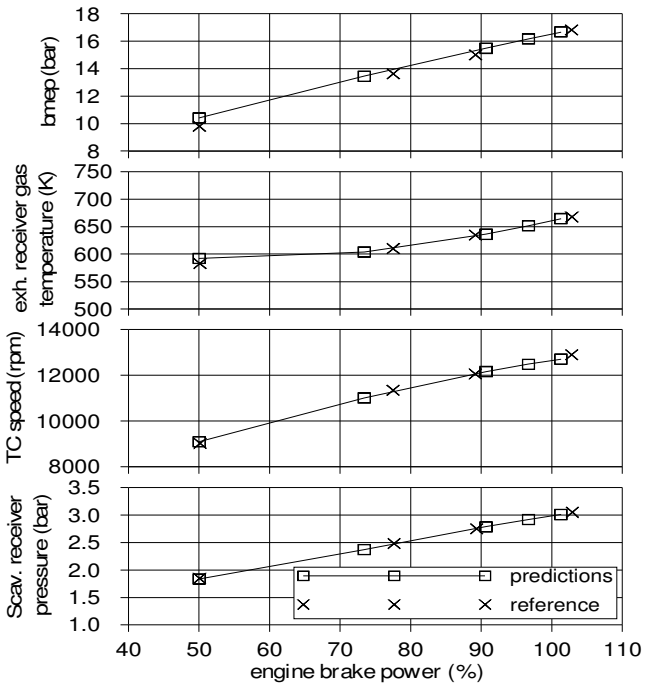

Fig. 4 Simulation results under steady state engine operating conditions and comparison to reference data taken from [13]

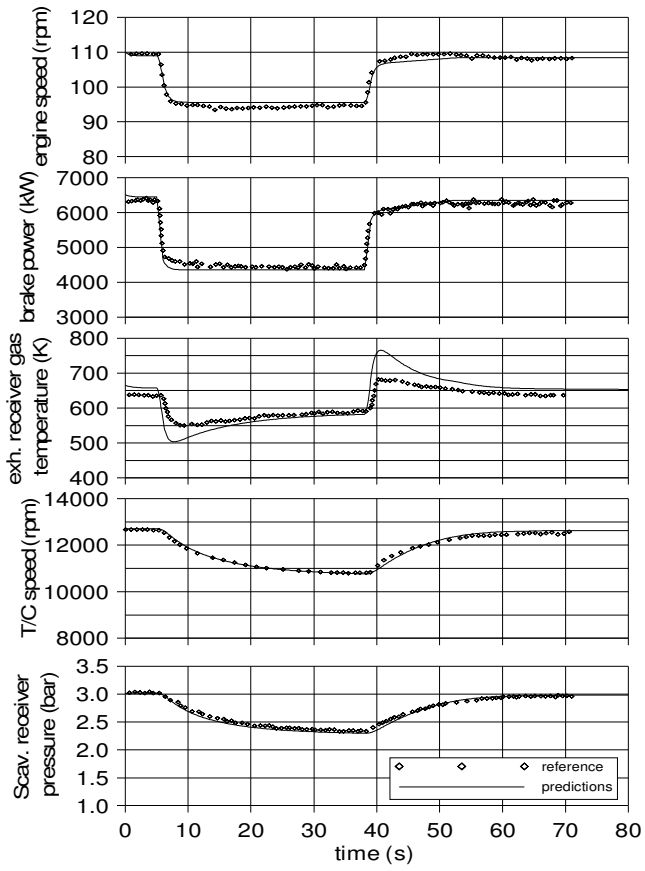

Fig. 5 Simulation under engine transient operating conditions and comparison to reference data taken from [13]

with two additional cylinders), which is directly connected to the ship propeller via the shafting system (i.e. gearbox is not installed). The main ship and propeller parameters are given in Table II.

TABLE II: SHIP & PROPELLER PARAMETERS

Ship Parameters		
Size (at scantling draught)	55000	dwt
Length overall	190	m
Length between perpendiculars	183	m
Breadth	32.26	m
Draught (scantling)	12.7	m
Draught (design)	11.5	m
Mass	$6.358\ 10^6$	kg

Propeller Parameters		
Diameter	6.5	m
Number of blades	5	
Pitch to diameter ratio	0.665	
Area ratio	0.57	

Slight modifications in the engine model input data, which was already set up for the MAN B&W 4L60MC, were performed. Then, the calibrated engine model in conjunction to the rest of the propulsion system geometric data was used to set up the overall propulsion plant model.

A set of results including operating parameters of engine, propeller and ship, which was derived from the simulation of the operation of the above described ship propulsion plant during a time period of 600 s (10 min), are shown in Fig.6. During the first 60 s of the simulation run, the engine is operating at 80 rpm, which corresponds to a rack position value of 0.42 and ship velocity of 10 knots. It must be noted the rack position value of 1.0 corresponds to the maximum continuous rating of the engine. After the 60th s, there is a linear increase in the ordered engine speed from 80 rpm to 105 rpm at the 180th s. This causes the action of engine governor, which increases the rack position resulting in more fuel to be injected and burnt into the engine cylinders, thus producing more engine torque. That, in turn, increases the engine shaft speed faster than the ship velocity rises, and as a consequence, the propeller produced thrust exceeds the ship resistance, thus accelerating the ship from 10 knots at 60th s to 13.1 knots at 280 s. As it is clearly seen from Fig. 6, during the ship acceleration period, the engine air to fuel ratio reduces, resulting in the increase of exhaust receiver temperature, which is more pronounced at the initial part of the ship acceleration period. That is owing to the slower response of the turbocharger system and the delivery of inadequate amount of air to the engine cylinders. However, after the 120th s, where the turbocharger speed increases, more air mass flow is available and the slope of the exhaust receiver gas temperature exhibits an obvious reduction. During the ship acceleration period, the propeller advance coefficient decreases due to the fact that the propeller speed increases faster than the ship velocity does, resulting in the reduction of the engine propeller open water efficiency. In addition, the propeller is more heavily loaded, which is also indicated by the observed increase of the propeller non-dimensional torque and thrust coefficients and the real slip ratio.

The engine ordered speed is held constant at 105 rpm till the 360th s. Then, a linear reduction in the engine ordered speed is

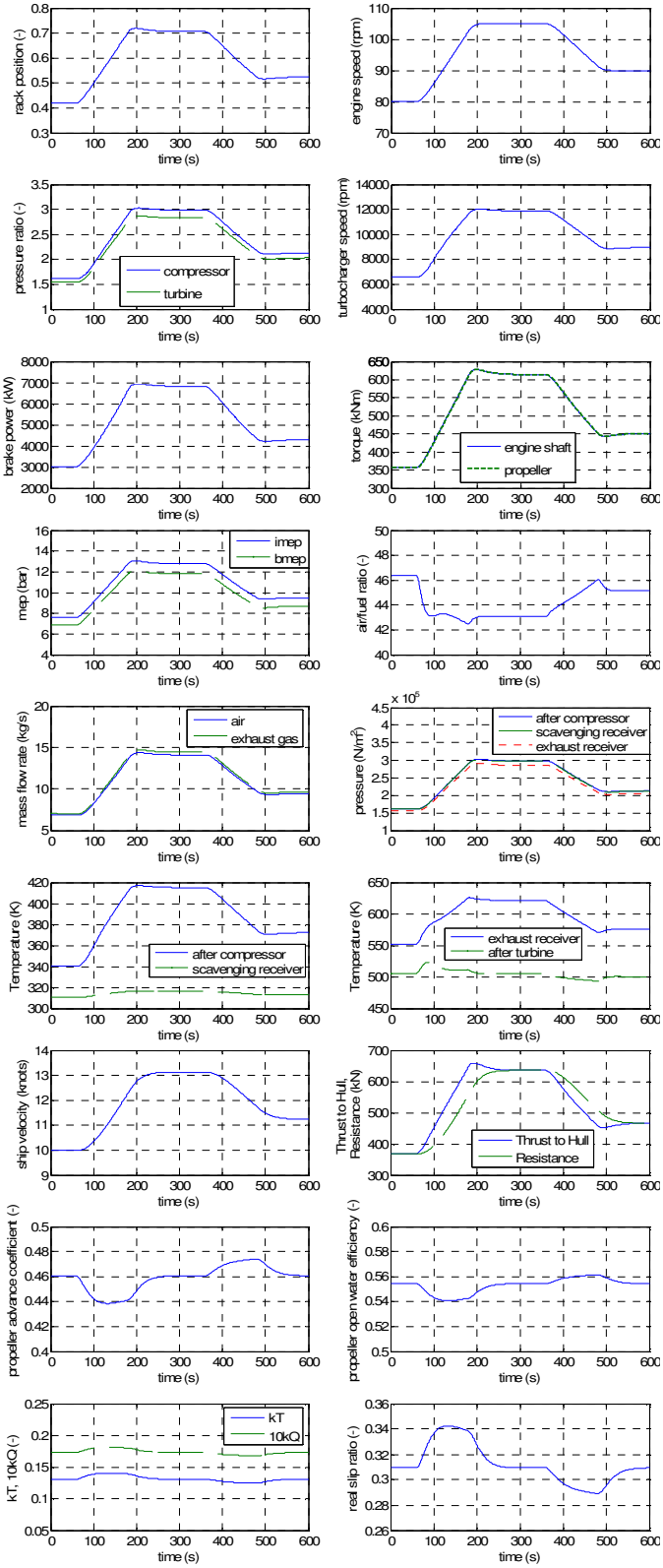

Fig. 6 Simulation results including engine, ship and propeller operating parameters

commanded from 105 rpm to 90 rpm at the 480th s. After the action of engine governor, the engine speed is reduced and the ship gradually decelerates to 11.2 knots. The engine air to fuel ratio increases as the fuel is reduced and at the same time due to the turbocharging system slower response, adequate amount

of air is still available. However, after the 500th s, the turbocharger speed and the compressor pressure ratio have been reduced enough so that the engine air mass flow rate also decreases, resulting in the reduction of the air to fuel ratio. The decrease of the mass of fuel injected into the engine cylinders leads to the engine speed reduction since for that period of the engine operation, the propeller absorbs greater amount of torque than the one delivered by the engine. In addition, due to the faster deceleration of the propeller speed than the respective one of the ship, the ship resistance exceeds the thrust delivered to the ship hull, thus causing the reduction of the ship velocity. During the ship deceleration period, the propeller advance coefficient increases resulting in a slight rise of the propeller open water efficiency. The propeller operates under lighter loading, as can be also deduced by the fall of real slip ratio and the non-dimensional torque and thrust coefficients.

As it is clearly deduced for the above described analysis of the transient simulation results, the overall propulsion plant modeling can be used in order to better understand the dynamic behavior of the propulsion plant as well as the engine-propeller-ship interaction.

V. Conclusion

The dynamic behavior of a bulk carrier propulsion plant was investigated using a model implemented in the computational environment MATLAB/Simulink. The main engine of the vessel propulsion plant, which is considered of the two-stroke marine Diesel type, is modeled using a quasi steady cycle mean value approach. First, the validation of the two stroke marine Diesel engine model under steady state and transient operating conditions was performed. Then, typical operating cases of the bulk carrier were simulated and the results containing engine, propeller and ship operating parameters were discussed.

The main findings derived from this work are summarized as follows.

The quasi steady mean value engine model is relatively simple compared to the more detailed zero or one-dimensional codes, requires small amount of input data and takes less computing time for execution. It adequately predicts the engine speed response. In order to represent with acceptable accuracy the turbocharger shaft speed and the scavenging receiver pressure responses during fast transients, the value of the turbocharger rotating parts polar moment of inertia, provided to the model as input, must be increased by an additional amount for taking into account the effect of the volume inertia of the engine scavenging and exhaust receivers and the turbocharging system piping. In such a case, additional data (experimental data or simulation results from more detailed models) are required in order to adjust the value of turbocharger inertia. Although the model can predict the exhaust receiver gas temperature under steady state conditions and during slow transients with adequate accuracy, it exhibits inefficiency to predict the exhaust receiver gas temperature variation during fast transients. In such cases, more detailed modeling of exhaust receiver, e.g. using open thermodynamic system approach, should be required.

The model can predict the dynamic behavior of the components of the ship propulsion plant and can be used to produce data that otherwise obtained using costly procedures. In that way, by analyzing the derived by the simulation ship-propeller-engine operating parameters response, the better understanding of the complex interactions between the subsystems can be obtained.

Nomenclature

A	area (m^2)
bsfc	brake specific fuel consumption (gr/kWh)
CQ	polynomial coefficients for k_Q calculation (-)
CT	polynomial coefficients for k_T calculation (-)
c_d	discharge coefficient (-)
c_p	specific heat at constant pressure (J/kgK)
c_v	specific heat at constant volume (J/kgK)
D	diameter (m)
F	thrust deduction (N)
f	friction factor (-)
I	polar moment of inertia (kgm^2)
J	propeller advance coefficient (-)
H_L	fuel lower heating value (J/kg)
h	specific enthalpy (J/kg)
k	coefficients, constants
k_p, k_i	engine governor proportional and integral constants
k_Q, k_T	propeller non-dimensional torque and thrust coefficients
m	mass (kg)
$m_{f,cy}$	mass of injected fuel per cylinder and per cycle (kg)
$\dot{m}$	mass flow rate (kg/s)
N	rotational speed (rpm)
P	power (W)
p	pressure (N/m^2)
pr	pressure ratio (-)
$\overline{p}$	mean effective pressure (bar)
Q	torque (Nm)
R	gas constant (J/kgK), resistance (N)
rev_{cy}	revolutions per cycle (-)
SR_R	propeller real slip ratio (-)
T	temperature (K), thrust (N)
t	time (s), thrust deduction coefficient (-)
u	specific internal energy (J/kg)
v	velocity (m/s)
V_A	propeller speed of advance (m/s)
V_D	displacement volume (m^3)
V_S	ship velocity (m/s)
V_u	circumferential propeller velocity (m/s)
w	ship wake fraction (-)
x_r	rack position (-)
z_{cyl}	number of engine cylinders (-)
z_P	number of propeller blades (-)
Greeks	
α	propeller advance angle (rad)
α_T	turbine flow coefficient (-)
γ	ratio of specific heats (-)
Δp	pressure drop (N/m^2)
ε	effectiveness (-)
ζ	proportion of the chemical energy of the fuel contained in the exhaust gas (-)
η	efficiency (-)
η_{ex}	correction factor for the temperature of the exhaust receiver (-)

ρ	density (kg/m^3)
ϕ	crank angle (deg)

Subscripts

AC	air cooler
atm	ambient
b	brake
C	compressor
comb	combustion
cy	cycle
cyl	cylinder
d	downstream
E	engine
ER	exhaust receiver
e	exhaust gas, exhaust valve
eff	effective
ep	exhaust pipe
eq	equivalent
ew	entrained water
f	fuel, friction
geo	geometric
hydro	hydrodynamic
i	indicated, intake ports
MCR	maximum continuous rating
max	maximum
o	initial conditions
P	propeller
S	ship
SC	scavenging receiver
Sh	shaft
sw	sea water
TC	turbocharger
T	turbine
w	cooling water
α	air

Abbreviations

MCR	maximum continuous rating

REFERENCES

[1] E. G. Faber, "Some Thoughts on Diesel Marine Engineering", SNAME Transactions, Vol. 101, (1993), pp. 537-582.

[2] R. L. Harrington (Ed.), *Marine Engineering*, SNAME, 1992.

[3] L. Guzzella and Ch. H. Onder, *Introduction to Modeling and Control of IC Engine Systems*, Springer, 2007.

[4] L. Eriksson, "Modeling and Control of Turbocharged SI and DI engines", Oil & Gas Science and Technology-Rev. IFP, Vol.62, No. 4, (2007), pp. 523-538.

[5] R.S. Benson, (edited by J.H. Horlock and D.E. Winterbone), *The Thermodynamics and Gas Dynamics of Internal Combustion Engines Vol. II*, Clarendon Press, 1986.

[6] J. B. Woodward and R. G. Latorre, "Modeling of Diesel Engine Transient Behavior in Marine Propulsion Analysis", SNAME Transactions, Vol. 92, (1984), pp. 33-49.

[7] E. Hendrics, "Mean Value Modeling of Large Turbocharged Two-Stroke Diesel Engines", SAE, (1989), Technical paper No. 890564.

[8] G. P. Theotokatos, "A Modelling Approach for the Overall Ship Propulsion Plant Simulation", 6th WSEAS International Conference on System Science and Simulation in Engineering (ICOSSSE'07), November 21-23 2007, Venice, Italy.

[9] J. Zhu, (2008), "Modeling and Simulating of Container Ship's Main Diesel Engine", Proceedings of the International MultiConference of Engineers and Computer Scientists, (IMECS 2008), March 19-21 2008, Hong Kong, Vol II, pp. 1980-1984.

[10] G. P. Theotokatos, "A Comparative Study on Mean Value Modelling of Two-Stroke Marine Diesel Engine", WSEAS International Conference on Maritime and Naval Science and Engineering, September 24-26 2009, Brasov, Romania.

[11] N. Xiros, *Robust Control of Diesel Ship Propulsion*, Springer, 2002.

[12] J. Klein Wood, Ph. Boot and B. J. ter Riet, "A Diesel Engine Model for the Dynamic Simulation of Propulsion Systems", Schip en Werf de Zee, January 1993.

[13] M. Larmi, "Transient Response Model of Low-Speed Diesel Engine in Ice-Breaking Cargo Vessels", Dr. of Technology Dissertation, Acta Polytechnica Scandinavica, Helsinki, Finland, ISBN 9516663788, 1993.

[14] N. P. Kyrtatos and I. Koumbarelis, "Performance Prediction of Next-Generation Slow Speed Diesel Engines during Ship Manoeuvers", Trans IMarE, Vol. 106, Part 1, (1994), pp. 1-26.

[15] X. Tauzia, P. Chesse, J. F. Hetet, G. Grosshans and L. Mouillard, "Study of the transient behaviour of a sequentially turbocharged medium speed diesel engine", Journal of Power and Energy, Institution of Mechanical Engineers, Vol. 212, Part A, (1998), pp.185–196.

[16] N. P. Kyrtatos, P. Theodossopoulos, G. Theotokatos and N. Xiros, "Simulation of the overall ship propulsion plant for performance prediction and control", MarPower99 Conference, The Institute of Marine Engineers, Newcastle upon Tyne, U.K., 1999.

[17] N. P. Kyrtatos, G. Theotokatos, N. Xiros, K. Marek and R. Duge, "Transient Operation of Large-bore Two-stroke Marine Diesel Engine Powerplants: Measurements and Simulations", 23rd CIMAC World Congress, Hamburg, Germany, 2001.

[18] N. P. Kyrtatos, G. Theotokatos and N. Xiros, "A Virtual Experiment Tool for Marine Diesel Engine Powerplant Analysis", 10th International Congress of the International Maritime Association of the Mediterranean (IMAM 2002), May 13-17 2002, Rethymnon, Crete, Greece.

[19] G. Benvenuto and U. Campora, "Dynamic Simulation of a High Performance Sequential Turbocharged Marine Diesel Engine", International Journal of Engine Research, Vol. 3, No. 3, (2002), pp.115-125.

[20] U. Campora and M. Figari, "Numerical Simulation of Ship Propulsion ransients and Full Scale Validation", Proceedings of Institution of Mechanical Engineers, Part M, Journal of Engineering for the Maritime Environment, Vol. 217, (2003), pp. 41-52.

[21] P. Chesse, D. Chalet, X. Tauzia, J. F. Hetet and B. Inozu, "Real-Time Performance Simulation of Marine Diesel Engines for the Training of Navy Crews", Marine Technology, Vol. 41, No. 3, (2004), pp. 95-101.

[22] G. A. Livanos, G. N. Simotas and N. P. Kyrtatos, "Tanker Propulsion Plant Transient Behavior during Ice Braking Conditions", 16th International Offshore and Poral Engineering Conference (ISOPE 2006), San Franscisco, USA, 2006.

[23] H. Grimmelius, E. Mesbahi, P. Schulten and D. Stapersma, "The use of Diesel engine simulation models in ship propulsion plant design and operation", CIMAC Congress 2007, Vienna, Austria, Paper No. 227., 2007.

[24] H. Klein Woud and D. Stapersma*, Design of Propulsion and Electric Power Generation Systems*, IMarEST, 2002.

[25] *Quick Guide to Propulsion Packages,* MAN B&W DIESEL A/S, 2000.

[26] E. Meier, "A Simple Method of Calculation and Matching Turbochargers", BBC Brown Boveri & Company Ltd, Publication No. CH-T 120 163 E.

[27] J. B. Heywood, *Internal Combustion Engines Fundamentals*, McGraw Hill, 1988.

[28] N. Watson and M. S. Janota, *Turbocharging the Internal Combustion Engine*, Macmillan Press, 1982.

[29] K. Heim, "Existing and Future Demands on the Turbocharging of Modern Large Two-stroke Diesel Engines", 8th Supercharging Conference, 2002.

[30] E. V. Lewis (Ed.), Principles *of Naval Architecture, Vol. II: Resistance Propulsion and Vibration*, SNAME, 1988.

[31] *Basic Principles of Ship Propulsion*, MAN B&W Diesel A/S, Publication No. p.254-04.04.

[32] C. J. Rubis and I. R. Hurper, "Ship Propulsion Dynamics Simulation, Control and Dynamic Systems", Academic Press, 1982, pp. 317-360.

[33] *Optimization Toolbox User's Guide Version 3.1.2*, The MathWorks Inc., 2007.

[34] *L60MC Mk5 Project Guide*, MAN B&W Diesel A/S, 1996.